

# Lab Characterization of the LISA Pathfinder Optical Metrology System

---

**Keeley Criswell**  
**Adviser: Martin Hewitson**  
**8/11/2014**

LISA Pathfinder (LPF), set to launch in 2015, is designed to test technologies that can be used in future space-based, gravitational-wave observatories. LPF contains an Optical Metrology System (OMS) that is used to measure the relative distance between the test masses. The OMS of the LISA Pathfinder currently has a ground model located in Hannover, Germany for testing of the system and system controls before launch. Currently, the system is being changed from analog to digital.

Abbreviations:

Control and Data System: CDS  
Differential Wavefront Sensing: DWS  
Discrete Fourier Transform: DFT  
Frequency Interferometer:  $X_F$   
LISA Pathfinder: LPF  
Measurement Interferometer for Displacement of TM1 relative to the OB:  $X_1$   
Measurement Interferometer for Relative Displacement between TM1 and TM2:  $X_{12}$   
Optical Bench: OB  
Optical Metrology System: OMS  
Optical Path Length Difference: OPD  
Piezoelectric Actuator: piezo  
Reference Interferometer:  $X_R$   
Test Mass: TM  
Test Mass 1: TM1  
Test Mass 2: TM2

# 1 – Introduction

Gravitational waves were first predicted by Albert Einstein in his Theory of Relativity. While it is widely accepted in the scientific community that they exist, they are extremely difficult to detect. Currently, major observatories include LIGO Livingston, LIGO Hanford, GEO 600, and VIRGO. Despite their operation, and the continued improvement of technology sensitivity, gravitational waves have yet to be directly detected.

The strongest gravitational waves come from the most massive objects – coalescing binary black holes and coalescing neutron stars. These binary systems orbit at low frequencies for years. However, as they approach merger, they move faster, emitting gravitational waves at higher frequencies. Currently, ground-based observation systems are only able to observe these high-frequency gravitational waves. Because these waves are only emitted for a short period of time – minutes – the ground-based observatories only have a small window for detection. Besides this, the most massive systems orbit at lower frequencies than less-massive systems. Sometimes, the objects in the system are so large that they merge before they can emit GWs in the audio-band, the frequencies that ground-based systems can detect.

For these reasons, A space-based observation system would have a significantly larger chance of observing gravitational waves because it can observe low frequencies, giving it much more of an opportunity for observation. Currently, there are plans for a gravitational wave detector in space called eLISA. As a precursor to the eLISA mission, LPF is planned to launch next year.

LISA pathfinder is a European Space Agency mission designed to test new gravitational-wave-detecting technology in space. While there are already gravitational-wave detectors on earth, this will be the first time that the technology is used in space. The technology aboard LPF Pathfinder is vital for any space-based attempt to observe gravitational waves. The ultimate goal is to send a full-scale detector, for example, eLISA, into space after LPF mission.

LPF will consist of one spacecraft containing two test masses. Once in space, these test masses will be in a near-perfect gravitational free-fall, separated by only a few centimeters. In order to detect gravitational waves, precise detection and measurement of any test-mass motion is necessary. These measurements will be made by the Optical Metrology System, or OMS. The purpose of the OMS is to detect any relative movement of the test masses and send that data back to scientists on Earth who will then analyze the movements.

Set for launch in 2015, LPF is currently in its final stages of preparation to be launched. The operational phase of the pathfinder is supposed to last about 9 months.

## 2 – The Optical Metrology Ground System

The OMS on board LPF is used to measure the relative positions of the test masses and to detect any minute changes in their positions. The setup utilizes an optical bench, complete with beam splitters, mirrors, and interferometers; lasers that are directed by fibers; and a phasemeter. The system will be responsible for passing this information on to the Data Management Unit which will calculate the actual positions and angular orientation of the test masses and report this information back to the scientists on the ground.

Since the actual OMS cannot be fully tested on the ground (as the test masses need to be in gravitational free fall), a ground, engineering model of the OMS exists for pre-launch tests. Before the launch, the technology within the system needs to be tested so that any necessary changes can be made while the OMS is still easily accessible. Pre-launch testing also allows for information to be gained about the noise affecting the system and how to best optimize noise-control loops. Generally, with space-based missions, multiple versions of a device are built over time, often leading to improvements in design.

### 2.1 – Test Masses

With the OMS ground setup, mirrors are used in place of the test masses onboard the LPF. The mirrors are attached to piezoelectric actuators, allowing the mirrors to be moved in a way similar to how the test masses will move in space. This means that they can be moved both longitudinally and angularly, enabling a proper testing of the technology [1]. Since the interferometers on board the LPF need to measure any test mass motion, be it longitudinal or angular, the piezoelectric actuators allow for accurate experiments to be conducted on the engineering model.

Each of the test mass mirrors is connected to three piezoelectric actuators. By adjusting one of these piezos, it is possible to move each of the mirrors a certain way. See section 4.1 for more information.

### 2.2 – Interferometers

In addition to the mirrors, the OMS has four interferometers installed on its optical bench. One of the interferometers is used to measure changes in distance between the first mirror and the optical bench. This is one of the two measurements that will need to be made of the test masses once LPF is launched. Another interferometer is used to measure the changes in distance between the two test masses – on the engineering model, test mirrors. The other two are used to measure fluctuations in the laser frequency (which are indistinguishable from test mass motion) and optical path-length changes originating in the beam paths prior to the optical bench, respectively.

$X_R$  is the reference interferometer. Its main purpose is to act as a reference for the test-mass measurements and OPD loop. Because this interferometer is located completely on the optical bench, it provides a stable reference measurement by measuring optical path-length fluctuations that are common to all of the interferometers [5]. The phase provided by  $X_R$  is subtracted from the phase measured by the other interferometers to cancel the optical-path-length

variations [6]. The OPD loop is used for suppression of residual fluctuations and any non-linear effects. Rather than subtraction, the OPD loop uses the signal from  $X_R$  to suppress these optical path-length fluctuations [6]. The OPD loop suppresses the fluctuations by moving a piezoelectric actuator located on the modulation bench to adjust the optical path length of the measurement beam [1].

The frequency interferometer, denoted  $X_F$ , measures the frequency noise of the laser. There is an intentional path-length difference of the two laser beams in this interferometer. The difference of 38 cm allows for the calibration of the phase to frequency [1]. The interferometer measures phase changes that are used to compute the frequency fluctuations that caused the changes [6].

$X_1$  measures the distance between TM1 and the optical bench. This measurement is then used to adjust the satellite, via micro-Newton thrusters, so that TM1 remains in its centered position [2]. Since the optical bench is attached to the pathfinder satellite, this measurement tells where the test mass is in relation to the satellite. Since the test mass should not hit the inside wall of the test-mass housing, it is necessary to move the satellite slightly in relation to the test mass motion. A centered test mass also yields the best noise performance of the system. The thrusters maintain the centering of TM1 with respect to the test-mass housing [7].

Lastly, while  $X_1$  deals with the motion of TM1,  $X_{12}$  measures the differential motion of TM1 and TM2. These measurements are important because it leads to the main signal for the experiments, the differential forces that affect TM1 and TM2 [2]. They are also important because they are used in maintaining the position of TM2 relative to TM1. The position is maintained by electrostatic forces applied by electrodes surrounding TM2.

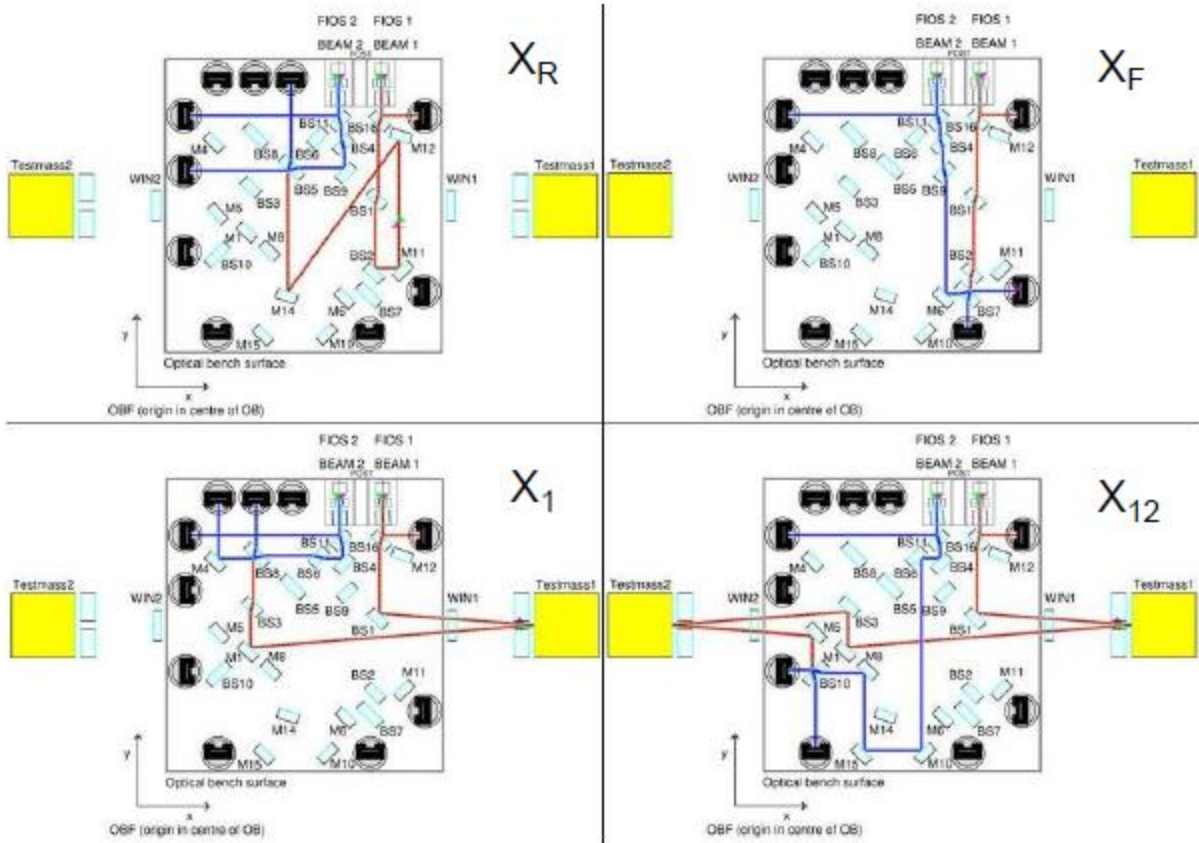


Figure 2.1: Here are schematics for the different interferometers that are part of the OMS.  $X_R$  is the Reference Interferometer,  $X_F$  is the Frequency Interferometer,  $X_1$  finds the distance between the optical bench and TM, and  $X_{12}$  finds the differential motion between the two test masses. [1]

## 2.3 – Laser

The laser used on the OMS engineering model is an InnoLight, Mephisto 500. This laser has a wavelength of 1064 nm [3]. The system contains two actuators – a fast actuator and a slow actuator. The fast actuator, operating with a bandwidth of roughly 100kHz, changes the laser frequency by moving a piezo on the last crystal [1][9]. The slow actuator, operating with a bandwidth around 1 Hz, adjusts the frequency by adjusting the temperature of the laser [1][9]. These two actuators are used in the frequency-control loop. Some transfer-function measurements with the fast control loop can be seen in section 3.2.1

When the beam reaches the modulation bench, it is split into two beams – a measurement beam and a reference beam. These beams are then used in the interferometers on the optical bench.

## 2.4 – Control Loops

When a system is designed to make measurements, those measurements need to be made with a certain level of precision. Even when a system is optimally designed, it still has to

contend with noise. Noise, which comes in countless forms, negatively affects the precision of a system. When left unchecked, it often renders measurements unreadable or useless. Therefore, these noise sources need to be controlled.

One way of reducing the noise on a system is through the use of control loops. LPF needs to achieve a precision of a few picometers in the measurement bandwidth (1-30 mHz) [4]. For this, several control loops are used to keep it operating within a certain noise margin. Two of these control loops, the OPD loop and the frequency loop, will be discussed in this paper.

### 2.4.1 – The Frequency Loop

Although  $X_1$ ,  $X_{12}$ , and  $X_R$  were designed to have no optical-path-length difference between their two beams, the reality is that some unavoidable differences can occur, either due to manufacturing tolerances, or due to absolute test mass positioning. Some of the largest contributors that affect these differences are optical fibers, fiber couplers, and laser modulators [6]. Because the path length difference causes coupling of laser frequency noise, it is necessary to mitigate the effect caused by the path-length differences [8].

To mitigate the noise,  $X_F$  and  $X_R$  are used in a frequency control loop. They are not used directly; however,  $X_F - X_R$  is used as the input.  $X_R$  shows the amount of path-length-difference that affects measurements and  $X_F$ , with its known path-length difference of 38 cm, can be used to show the amount of noise that occurs per unit of length. As with the other interferometers,  $X_R$  is subtracted from  $X_F$  [1][10]. When  $X_R$  is subtracted from  $X_F$ , this mitigates any error caused by the common-mode environmental noise, that which is measured with  $X_R$  [10]. Now,  $X_F$  gives only the noise caused by frequency.

There are two frequency control loops – a fast loop and a slow loop. The slow frequency control loop deals with laser frequency that has a band-width less than 1 Hz, and the fast loop deals with those up to about 10 Hz (on time-scales longer than 1 second). The slower frequency fluctuations are mostly associated with the temperature of the laser crystal [1]. The faster frequency fluctuations are associated with the piezo on the laser head [1]. Below, graphs are shown that depict the noise decrease that comes about with the implementation of the frequency control loop.

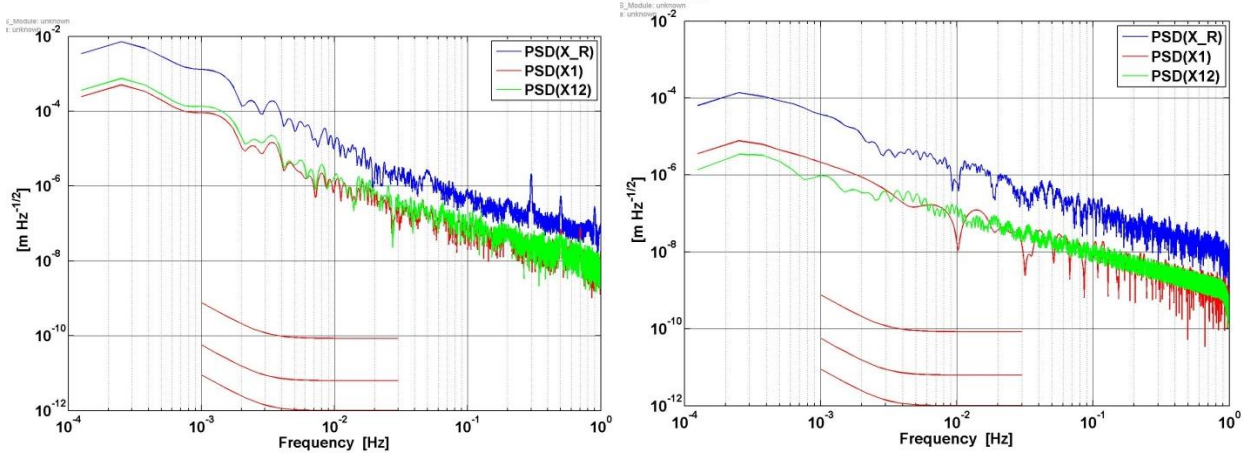


Figure 2.2: The graph on the left shows a noise measurement without control loops. The top red curve shows the LPF mission goal, and the middle red curve shows the interferometer goal; the bottom red curve is the contribution goal for each individual noise source [1][9]. The graph on the right shows a noise measurement with only the frequency control loop. While it is evident that this loop reduces noise, it is also apparent that this in itself does not reduce the noise nearly enough for optimal performance.

### 2.4.2 – The Optical Path Length Difference Loop

The OPD loop makes use of  $X_R$  to measure and cancel the noise related to phase fluctuations. Phase refers to the offset of two sine waves reaching a sensor (see figure 3.2). The phase differences that affect measurement are caused when differences in path length allow one sine wave to reach the sensor before another sine wave. When this occurs, the sine waves are said to be out of phase.

Because the modulation bench is unstable, phase fluctuations occur.  $X_R$  is used to measure these variations and relay that information to the OPD loop [8]. When activated, the OPD loop allows a signal from  $X_R$  to go to a piezo-actuated mirror on the modulation bench [1][8]. The signal tells the mirror, which is located along the reference beam, to move a certain way to correct for the current phase shift [1]. The effects of this loop can be seen in Figure 3.3.

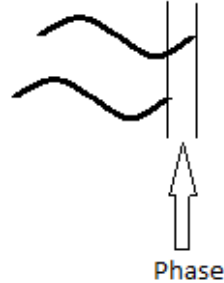


Figure 3.2: This figure depicts a phase difference between two sine waves.

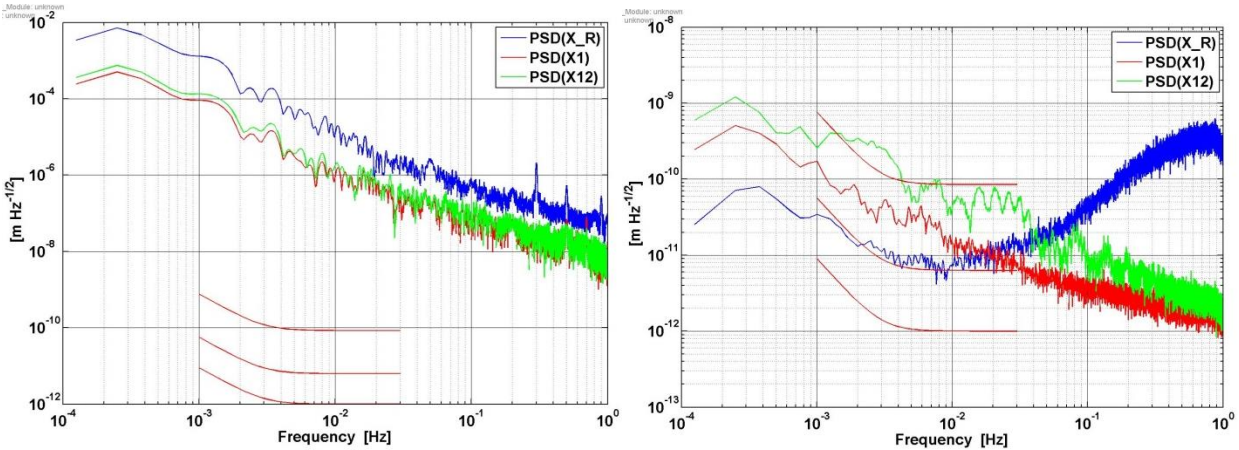


Figure 3.3: The graph on the left shows a noise measurement without control loops. The top red curve shows the LPF mission goal, and the middle red curve shows the interferometer goal; the bottom red curve is the contribution goal for each individual noise source [1][9]. The graph on the right shows a noise measurement with only the OPD loop. While it is evident that this loop reduces noise, the OPD loop in itself does not reduce the noise enough for optimal performance. Therefore, other loops must be activated.

## 2.5 – Contrast

A photodiode's contrast is the measure of the overlap of the beams that comprise the photodiode. The more the two beams overlap, the higher the contrast will be. It is necessary to achieve a contrast as high as possible because this indicates well-aligned beams. The more aligned the beams, the more sensitive the measurement of the optical phase. A major contributor to the contrast levels is the power of the laser beam. Because the laser beam is directed through several fibers before entering the optical bench, it is important that the beam hits each fiber head as directly as possible. This way, the photodiode reads a high power from the laser beam and, as a consequence, the contrast is also high.

One can position a beam directly before it enters a fiber. This is accomplished via mirrors, placed in front of the fiber heads, which reflect the beam and direct it into the fiber. These mirrors are adjusted manually via screws around each of the mirrors. By turning the screws, it is possible to shift the mirror to the left, right, up, or down, thus slightly changing the direction of the beam.

To measure the beam intensity, and position the mirrors, it is necessary to use a photodiode connected to an oscilloscope. Then, one can gradually adjust the mirrors until the largest possible value has been reached, around 13 volts. The power of the laser exiting the fiber can be checked with a Powermeter. Once the power is reasonable and cannot be maximized further with the mirrors, then the contrast can again be checked.

Before positioning the mirrors, the contrast was well below 5% for the bulk of the photodiodes. However, after adjusting the mirrors, the contrast jumped to about 75% on the main photodiodes and around 40% on some of the other photodiodes.

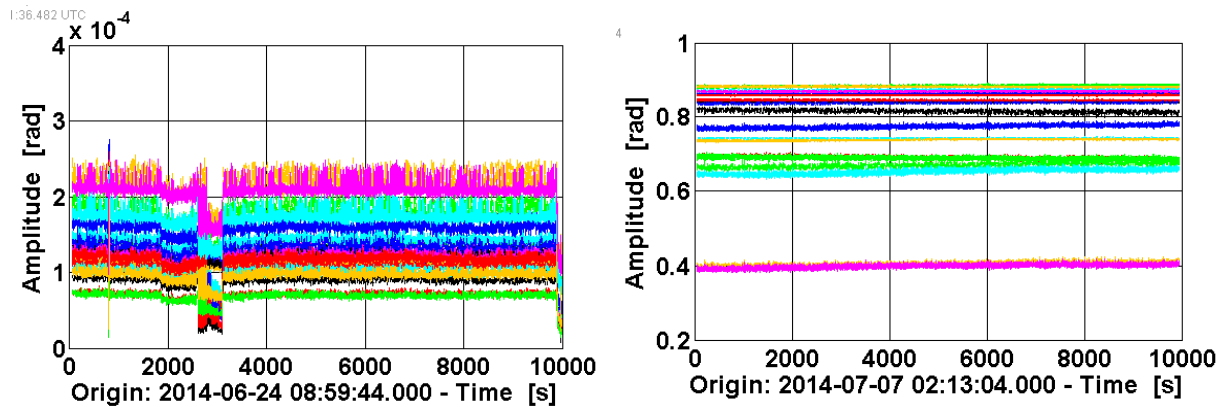


Figure 3.1: Shown are two contrast plots taken at different times. The one on the left was taken before adjusting the mirrors, and the one on the right was taken after adjusting the mirrors. There is a sharp increase in contrast between the two measurements.

## 3 – Movement of the Test Masses

As mentioned in section 2.1, each of the test masses is connected to one three-axis piezoelectric actuator that allows for movement in three directions. Each piezo moves the TM a certain way, allowing movement along three axes. The TMs are able to move longitudinally, and in two rotational directions. Figure 3.1 depicts the possible TM movements along the various axes. During experimentation, the directions of movement are referred to as  $x$ , in the longitudinal direction;  $\eta$ , in one of the angular directions; and  $\varphi$ , in the other angular direction.

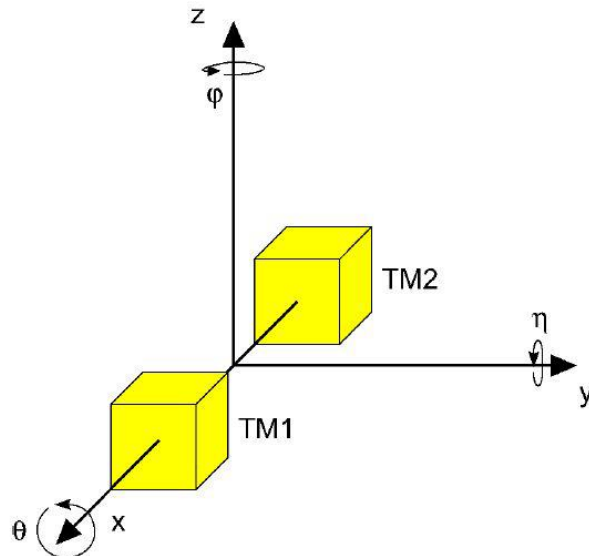


Figure 3.1: Each of the test masses is able to move in three directions,  $x$ ,  $\eta$ , and  $\varphi$ , along the X, Y, and Z axis, respectively.

### 3.1 – Digital Setup

It is considered good practice to implement several different versions of a system before a major project. With each additional system, methods improve, and the overall capabilities of the system become better in one way or another. This method of testing is being implemented with the OMS ground system.

The initial OMS Engineering Model utilized an analog setup. This means that analog components were used to run the control loops and move the test masses. One of the main drawbacks to this system is that it is not very flexible and the movement of the test masses is a hassle and imprecise [1]. A digital setup, however, will allow greater accuracy and flexibility within the system. For example, with a digital setup, a digital control loop can be used to counter thermal drift so that measurements can be performed over several weeks rather than several days [1].

As part of the new digital setup, the test mass motion will be dictated via computer software. By typing a distance or angle into the CDS software, a driver will move the TM by that amount. By reading and implementing a programmed matrix, the software is programmed

to know how much voltage to give each piezo to achieve the desired movement. The software uses a matrix calibrated for each of the two TMs.

### 3.2 – Calculating Motion

A MATLAB program is used to calculate the values of the matrix, called P (shown in Equation 3.1). In order to run the program, a suitable amount of data (several hours, preferably overnight or over a weekend when there are fewer disturbances in the lab) is required. To acquire the data, signals should be injected into the piezos at different frequencies to move one of the test masses. The measurements from this should then be analyzed.

$$\begin{matrix} & \text{real world : CDS world} \\ \begin{bmatrix} x \\ \eta \\ \varphi \end{bmatrix} = \begin{bmatrix} a_1 & a_2 & a_3 \\ b_1 & b_2 & b_3 \\ c_1 & c_2 & c_3 \end{bmatrix} : \begin{bmatrix} X \\ Y \\ Z \end{bmatrix} \leftarrow \begin{matrix} 1 \text{ mHz} \\ 3 \text{ mHz} \\ 5 \text{ mHz} \end{matrix} \end{matrix}$$

Equation 3.1: Shown is the matrix P which is used in part to determine how much to move each piezo to dictate certain movements of the test masses. The CDS program converts the matrix it is given to distances in the various directions.

$$[x_1^{1\text{mHz}} \quad x_2^{3\text{mHz}} \quad x_3^{5\text{mHz}}] = a_1 X^{1\text{ mHz}} + a_2 Y^{3\text{ mHz}} + a_3 Z^{5\text{ mHz}}$$

Equation 3.2: This equation stems from the matrix in Equation 3.

$$a_1 = \frac{x_1^{1\text{mHz}} [\text{m}]}{X^{1\text{mHz}} [\text{counts}]} = ?$$

Equation 3.3: The values need to be divided by the number of counts used during the experiment. This Equation is derived from Equation 3.2.

The first step of the analyzing process is to window the data function. If a DFT were to be performed on a sinusoidal signal, like that in this experiment, without performing a window function, the data will be incorrect [12]. Rather than showing a spike at one frequency, as expected, the graph will show something else entirely [12].

After the data has been windowed, a DFT can be completed without issues. The DFT must be completed for x, eta, and phi at each of the drive frequencies. In this particular experiment, the drive frequencies were 11 mHz, 13 mHz, and 15 mHz. These results are then divided by the number of counts used during the experiment. This gives results in meters/count or radians/count, depending if the DFT is for x (meters) or eta or phi (radians).

Next, the absolute value of the DTFs is computed to get the coefficient. This is followed by a scaling of the absolute values to get the value in m (or rad) rms (root mean square). The absolute values are scaled by  $\frac{\sqrt{2}}{\sum(\text{window values})}$ .

Lastly, the phase angle of the DFT is calculated and the sign of the phase angle is taken. This acquires the sign of the coefficient. This last step was added after the MATLAB program had been run and a matrix has been found. The first matrix was input to the CDS program, and it

did not work properly. This is because we were unable to compute a proper transfer function from the drive signal to the observed motion

Differential wavefront sensing is also a part of this process. More information can be found about DWS in section 3.3.

Once all the values of the matrix have been found, the matrix must be inverted. It is the inverted matrix that will be input to the CDS program. This is because when you multiply a matrix by its inverse, you get all 1s along the diagonal. These 1s allow the desired motion of the test mass, input to the CDS, to be the motion that the test mass makes.

### 3.3 – Differential Wavefront Sensing

DWS is a technique used to determine the angle of the test mass mirrors. It makes use of a quadrant photodiode and two interfering beams, one of which is a reference beam positioned to hit the photodiode in the center [1]. The reference beam will hit each quadrant of the photodiode at the same time since this beam has no angle. If the measurement beam hits the photodiode in a like manor, then there is no angle involved. However, when the measurement beam hits the photodiode at an angle, the beam will arrive at one half of the photodiode sooner than it will reach the other half [8]. This information can be used to calculate the angle at which the measurement beam comes, and, in the case of LPF, the angle of the test masses.

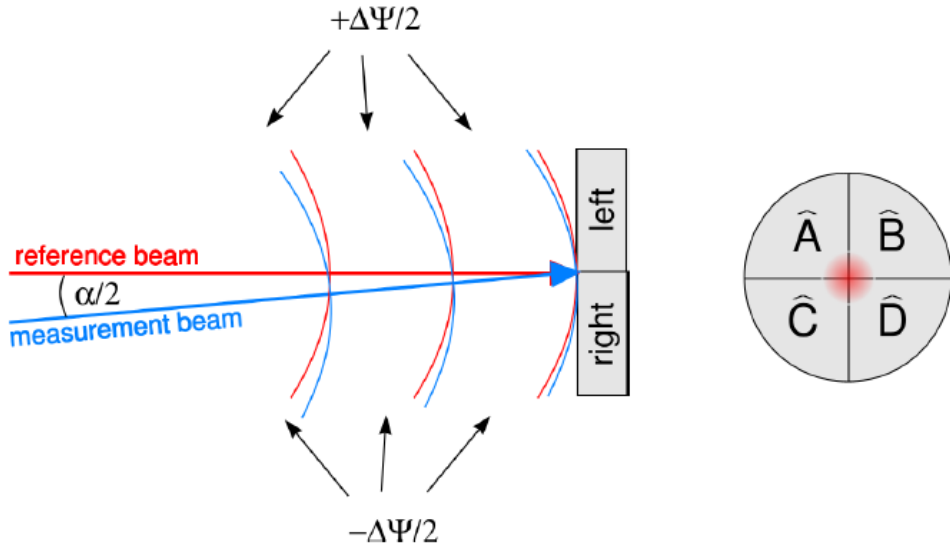


Figure 3.2: The left portion of this figure shows a schematic of what occurs to make DWS possible – when the measurement beam comes in at the angle shown, the light hits the right side of the photodiode sooner than it hits the left. This is then used to calculate the angle involved. The right portion of the figure depicts a quadrant photodiode. [8]

### 3.4 – Results

After the appropriate matrices have been found, a test should be run to test their accuracy. To run the test, certain frequencies should be injected into the system using the newly configured CDS system. In this case, frequencies of 11, 13, and 15 mHz were used. The expectation from

this test is that when a test mass is commanded to move in a certain direction, there will be little to no motion in one of the other two degrees of freedom. If this is the case, then the matrix was configured correctly.

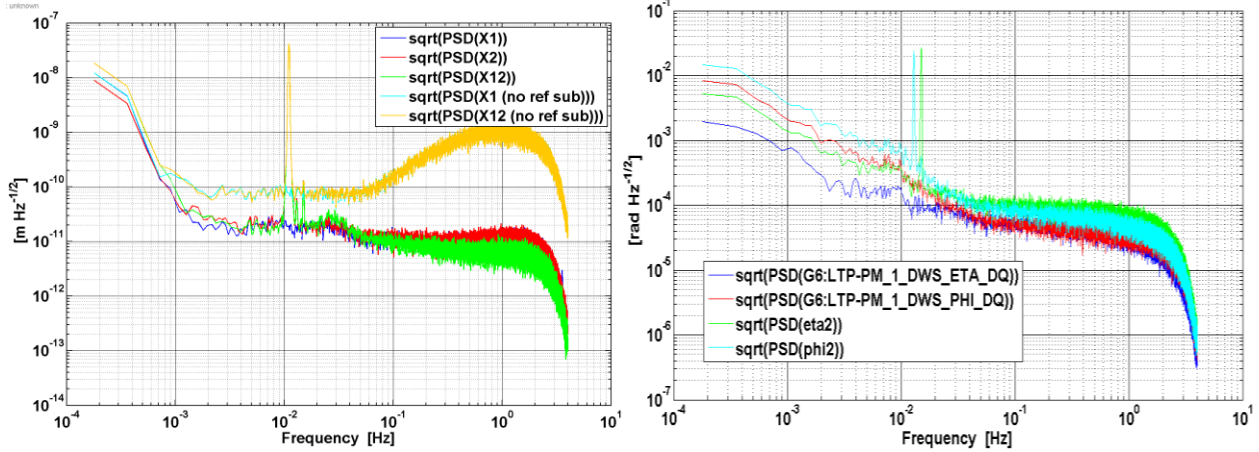


Figure 3.3: These graphs show the movement of TM1 in certain directions at certain frequencies. The traces on the left plot show a strong signal at 11 mHz indicating movement in the X direction. It also shows a small signal at 13 and 15 mHz, but this is likely due to a small amount of cross coupling and noise in the system and can be improved. The traces on the right plot depict a strong signal in the phi direction at 13 mHz and a strong signal in the eta direction at 15 mHz. These main spikes, and the lack of major spikes in other locations, were expected and show that the matrix is working properly. The graphs for TM2 are similar and it would be redundant to also show them.

Sources:

[1] – Andreas Wittchen. *Noise investigation on the LISA-Pathfinder optical bench ground setup*. Master's thesis. AEI Hannover, Max Planck Institute, 2013. 7, 8, 13, 14, 16, 54.

[2] – LPF Technology: Satellite and Test Mass Control. *Max Planck Institute for Gravitational Physics*. <https://www.elisascience.org/articles/lisa-pathfinder/lpf-technology/satellite-and-test-mass-control>.

[3] –Laser Factsheet. *Innolight*.

[http://www.innolight.de/fileadmin/user\\_upload/produktblatt\\_pdf/Produktblatt\\_Mephisto.pdf](http://www.innolight.de/fileadmin/user_upload/produktblatt_pdf/Produktblatt_Mephisto.pdf).

[4] – LISA Pathfinder factsheet. *European Space Agency*. 2013.

[http://www.esa.int/Our\\_Activities/Space\\_Science/LISA\\_Pathfinder\\_factsheet](http://www.esa.int/Our_Activities/Space_Science/LISA_Pathfinder_factsheet).

[5] – LPF Technology: The Ultra-Stable Optical Bench. *Max Planck Institute for Gravitational Physics*. <https://www.elisascience.org/articles/lisa-pathfinder/lpf-technology/ltp-optical-bench>.

[6] – Gerald Hechenblaikner, Vinzenz Wand, Michael Kersten, Karsten Danzmann, Antonio Garcia, Gerhard Heinzel, Miquel Nofrarias, Frank Steier. *Digital laser frequency control and phase stabilization loops for a high precision space-borne metrology system*. IEEE Journal of Quantum Electronics, Vol. 47, No. 5, p.p. 651 (2011). 652, 653  
<http://ieeexplore.ieee.org/stamp/stamp.jsp?tp=&arnumber=5738954>.

[7] – LPF Technology: Capacitive Actuation and Sensing. *Max Planck Institute for Gravitational Physics*. <https://www.elisascience.org/articles/lisa-pathfinder/lpf-technology/cap-actuation-and-sensors>.

[8] – Frank Steier. *Interferometry techniques for spaceborne gravitational wave detectors*. Ph.D. thesis, Laser Interferometry & Gravitational Wave Astronomy, AEI Hannover, MPI for Gravitational Physics, Max Planck Society, escidoc:24010, 2008. 90, 91, 92, 93.

[9] – Vinzenz Wand. *Interferometry at low frequencies: Optical phase measurement for LISA and LISA Pathfinder*. Ph.D. thesis, Leibniz Universität Hannover, 2007. 7, 25.

[10] – Antonio F. García Matín. *Minimisation of optical pathlength noise for the detection of gravitational waves with the spaceborn laser interferometer LISA and LISA Pathfinder*. Ph.D. thesis, Leibniz Universität Hannover, 2007. 54-61.

[11] – Felipe Guzmán Cervantes. *Gravitational wave observation from space: optical phase measurments for LISA and LISA Pathfinder*. PhD thesis, Max Planck Institute for Gravitational Physics (Albert-Einstein-Institute), 2009. 16, 109

[12] – Heinzel, G.; A. Rudiger; and R. Schilling. *Spectrum and spectral density estimation by the Discrete Fourier Transform (DFT), including a comprehensive list of window functions and some new*

*flat-top windows.* Max-Planck-Institute for Gravitational Physics (Albert-Einstein-Institute). Feb. 15,  
2002. 11